

Danny Arora and Daniel Burke Whelan

## Contents

4.1	<b>What Radiographic Views to Order?</b> .....	40
4.1.1	Anteroposterior Pelvic View .....	40
4.1.2	45° or 90° Dunn Views .....	40
4.1.3	Frog-Leg Lateral View .....	41
4.1.4	False-Profile View .....	41
4.2	<b>What Radiographic Parameters to Assess?</b> .....	41
4.2.1	Acetabular Depth .....	42
4.2.2	Acetabular Inclination .....	42
4.2.3	Acetabular Coverage .....	42
4.2.4	Acetabular Version .....	43
4.2.5	Femoral Head Morphology .....	43
4.2.6	Head-Neck Junction and Offset .....	43
4.2.7	Degree of Osteoarthritis (OA) .....	44
4.3	<b>Additional Imaging</b> .....	44
4.3.1	Fluoroscopy .....	44
4.3.2	Computed Tomography (CT) .....	45
4.3.3	Magnetic Resonance Imaging (MRI) .....	45
4.4	<b>The Interobserver and Intra-observer Reliability</b> .....	46
4.5	<b>Cost-Utility of Imaging for FAI</b> .....	46
	<b>Conclusion</b> .....	46
	<b>References</b> .....	47

Femoroacetabular impingement (FAI) is an increasingly recognized cause and one of many accepted causes for labral pathology of the hip, specifically in the young, active adult [1–3]. There have been a few reports on the correlation of FAI and the development of osteoarthritis of the hip secondary to the bony impingement and subsequent chondrolabral damage [1, 4].

FAI often presents with clinical signs of intra-articular hip irritation secondary to labral pathology in patients with groin pain. During the physical examination, the physician can further characterize the groin pain and perform special hip impingement tests, such as the flexion, adduction, and internal rotation (FADDIR) test, which is the most sensitive physical examination test for FAI [5]. The mainstay of diagnosing FAI as a cause of intra-articular hip pain is, however, via radiographic imaging. All other adjuncts are used to confirm the diagnosis. Some authors believe that adding an intra-articular injection helps with the accuracy of the diagnosis [6, 7]. Nonetheless, the diagnosis of FAI is predominantly radiographic.

Despite recent advances in the diagnostic evaluation, obtaining an accurate diagnosis can prove to be challenging; therefore, it is essential to introduce standardized and consistent radiographic views as well as parameters for their interpretation that can serve as a foundation for accurate diagnosis, disease classification, prognostication, and surgical decision-making [8].

---

D. Arora, MD, FRCS(C)  
D.B. Whelan, MD, MSc, FRCS(C) (✉)  
Department of Orthopaedic Surgery,  
University of Toronto Orthopaedic Sports Medicine,  
Toronto, ON, Canada  
e-mail: [WhelanD@smh.ca](mailto:WhelanD@smh.ca)

## 4.1 What Radiographic Views to Order?

There are many different views that have been described to help visualize and quantify different parameters of hip alignment, morphology, and position. Clohisy et al. [8] outlined a systematic approach to radiographic evaluation of hip dysfunction in the adult patient. The most commonly employed views are an anteroposterior (AP) pelvic view [9, 10], a 45° or a 90° Dunn view [12, 13], a frog-leg lateral view [11, 14], and a false-profile view [14, 15]. To improve diagnostic accuracy and disease classification, radiographs must be obtained with use of the same standardized imaging protocol. The techniques for obtaining each view will be outlined below.

### 4.1.1 Anteroposterior Pelvic View

The AP pelvic view is taken with the patient supine with their legs internally rotated 15° (Fig. 4.1). The tube-to-film distance should be 120 cm with the tube oriented perpendicular to the table [8]. The beam is directed vertically to the midportion of the pelvis, specifically midway from the superior border of the symphysis pubis and a line connecting the anterior superior iliac spines (ASISs) [10]. Pelvic tilt, inclination, and rotation should be taken into account when analyzing this view. If the pelvic inclination is adequate, the coccyx should be directly in line with

the symphysis pubis. Proper tilt is controlled by maintaining the distance between the tip of the coccyx and the superior border of the symphysis pubis at 1–2 cm [54]. Increased pelvic tilt or rotation has been shown to produce apparent retroversion in an anteverted hip [15]. Siebenrock et al. [15] published sex-specific values for pelvic tilt (referencing the distance between the superior aspect of the symphysis and the sacrococcygeal junction) and noted that an average distance of 32.3 mm was typical in men, as compared with 47.3 mm in women.

Recently, Pullen et al. [16] have shown variability in supine versus weight-bearing anteroposterior (AP) pelvic radiographs in their study of non-arthritic hips in adults with hip pain. They found significant variability with respect to pelvic tilt and radiographic measures of acetabular coverage, where the change from supine to weight bearing typically, but not uniformly, resulted in more posterior pelvic tilt and therefore decreased acetabular coverage. In the supine views, the anterior pelvic tilt was demonstrated, which resulted in increased acetabular coverage. This data brings into question the optimal position when obtaining an AP pelvic radiographic view.

### 4.1.2 45° or 90° Dunn Views

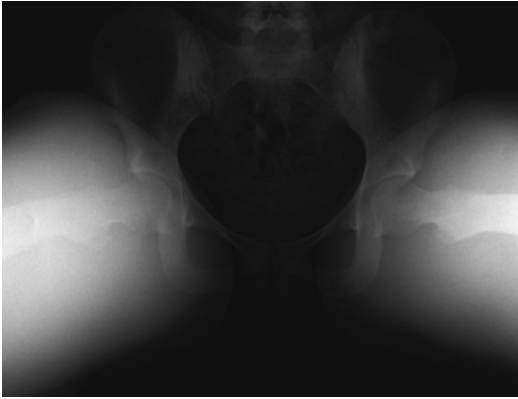
The 45° or 90° Dunn views are taken with the patient supine (Figs. 4.2 and 4.3). The affected leg is flexed 45° or 90° and abducted 20° with



Fig. 4.1 AP view



Fig. 4.2 45° Dunn view



**Fig. 4.3** 90° Dunn view



**Fig. 4.4** Frog lateral view

neutral rotation. The beam is directed at a midpoint between the symphysis pubis and a line between the anterior superior iliac spines (ASISs). The tube-to-film distance should be about 100 cm perpendicular to the table [8]. The Dunn views are best used to appreciate head sphericity, head-neck junction, and offset [8].

#### 4.1.3 Frog-Leg Lateral View

The frog-leg lateral view is taken with the patient supine, the affected limb flexed 30–40°, and the hip abducted 45° (Fig. 4.4). The heel of the affected limb should lean on the medial aspect of the con-

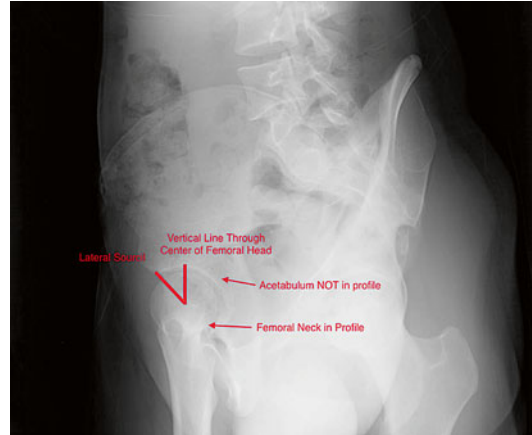


**Fig. 4.5** False profile view

tralateral knee. The beam is directed at a midpoint between the symphysis pubis and a line between the anterior superior iliac spines (ASISs) with the tube-to-film distance of 100 cm [8]. The frog-leg lateral view also profiles the femoral head sphericity, the head-neck junction, and the offset, keeping in mind that the greater trochanter can obscure this specific zone. It is important to note that in this view, the lateral of the proximal femur is visualized but it is not a lateral of the acetabulum, hence the use of a false-profile view for better acetabular assessment.

#### 4.1.4 False-Profile View

The false-profile view is taken with the patient in a standing position. The affected limb is against the cassette and the pelvis is rotated 65° in relation to the wall stand (Fig. 4.5). The foot on the affected side should be parallel to the cassette. The beam is centered over the femoral head with a tube-to-film distance of 100 cm [8]. In this view, anterior coverage of the femoral head is appreciated, as well as anterior or posterior acetabular wear [8].

## 4.2 What Radiographic Parameters to Assess?

Each of the above views provides specific information, from which many radiographic parameters are measured and used to establish the

diagnosis of FAI. A systematic approach when interpreting each view should aid the surgeon in his/her decision-making. As a general rule, the AP pelvic view provides the most information on acetabular bony morphology. The Dunn and the frog-leg lateral views highlight the morphological differences of the proximal femur, whereas the false-profile lateral views provide important acetabular morphological information.

### 4.2.1 Acetabular Depth

The AP pelvic view is most helpful in obtaining a general sense of acetabular bony morphology. One can also get an appreciation of acetabular depth. Using this view, the hips can be classified as being globally “overcovered” or as having a “deep socket” if they fall into two general categories: “coxa profunda,” [4] if the floor of the acetabular fossa lies at or medial to the ilioischial line (ICC=0.02; range=-0.72-0.44) [17], or “protrusio acetabuli,” if the femoral head sits medial to the ilioischial line (ICC=0.10; range=-0.57-0.49) [17]. In a recent study, Nepple et al. [18] found that the presence of coxa profunda can be a normal finding and has a limited role in diagnosing pincer-type FAI. To further assess femoral head overcoverage, they recommend investigating the following parameters: crossover sign, posterior wall sign, lateral center-edge angle, anterior center-edge angle, and acetabular inclination. These parameters help to further distinguish global overcoverage from localized areas where the acetabular margin may be prominent.

### 4.2.2 Acetabular Inclination

The Tönnis angle [19] is used to calculate the degree of acetabular inclination. It represents the horizontal orientation of the weight-bearing zone of acetabulum on an AP pelvic radiograph. It is measured by calculating the angle between a horizontal line at the most inferior aspect of the sclerotic acetabular sourcil parallel to the teardrop line and a line extending to the most

lateral edge of the sclerotic acetabular sourcil [19]. The normal range for this angle measurement is 0–10°. Values of >10° and <0° are considered to have increased and decreased inclination, respectively. In general, acetabuli with increased Tönnis angles are usually dysplastic and may be subject to structural instability, whereas those with decreased Tönnis angles are at risk for pincer-type femoroacetabular impingement [8] (ICC=0.70; range=0.48–0.83) [17].

### 4.2.3 Acetabular Coverage

The lateral center-edge angle (LCEA) of Wiberg [20] is the most common measure of acetabular coverage. Specifically, it is used to quantify the superolateral acetabular coverage and is best measured on an AP pelvic view. It is the angle between a line drawn perpendicular to the transverse axis of the pelvis and a line drawn from the center of the femoral head extending to the most superolateral point of the sclerotic acetabular sourcil (weight-bearing zone). An LCEA of <20° is considered as femoral head undercoverage or, traditionally, acetabular dysplasia [21–24]. An LCEA of >40° is found to be abnormal and defined as acetabular overcoverage or profunda, seen specifically in pincer-type FAI [21, 25–28]. When analyzing the reliability to interpret common radiographic findings of the adult hip by various observers, Carlisle et al. found that the LCEA was the most consistently assessed value between readers, with an excellent intra-rater observer (ICC=0.88; range = 0.85–0.91) and interobserver value (ICC=0.64; range=0.52–0.75) [29].

On a false-profile lateral view, the anterior center-edge angle of Lequesne [14] is calculated to assess the anterior femoral head coverage. It is the angle between a vertical line through the center of the femoral head and a line extending to the most anterior portion of the sclerotic acetabular sourcil. An angle of <20° can be indicative of anterior undercoverage, seen in entities like dysplasia [8] (ICC=0.38; range=0.26–0.53) [29].

#### 4.2.4 Acetabular Version

Acetabular version can also be investigated on the AP pelvic view. Acetabular anteversion is appreciated on the AP pelvic view, when the anterior portion of the anterior acetabular rim is superior and medial to the posterior rim and does not cross the posterior portion of the rim before reaching the lateral aspect of the sourcil. Less commonly, acetabular retroversion is seen when the anterior portion of the acetabular rim does cross the posterior portion of the rim before reaching the lateral edge of the sourcil. This has been described as the “crossover” sign [9] (ICC = 0.29; range = -0.25–0.59) [30]. True acetabular retroversion is characterized by global anterior overcoverage with corresponding posterior undercoverage and may result in isolated anterior impingement or combined anterior impingement with posterior coverage deficiency, leading to posterior instability. This morphology is different from focal cranial retroversion, which is characterized by localized overcoverage only at the cranial aspect of the acetabulum with normal posterior wall coverage. The presence of a posterior wall sign (the posterior wall of the acetabulum sits medial to the center of the femoral head [10]) (ICC = 0.20; range = -0.40–0.54) [17] and an ischial spine sign [31] (exaggerated size of the ischial spine projecting medial to the pelvic inlet (ilioischial line)) (ICC = 0.55; range = 0.20–0.74) [17] are radiographic findings on the AP pelvic radiograph that are suggestive of acetabular retroversion [31].

Zaltz et al. [32] demonstrated that acetabular retroversion remains difficult to identify and cannot be definitively diagnosed based on the presence of a “crossover” sign or ischial spine sign alone, even on a well-aligned pelvic radiograph with acceptable tilt and obliquity. Furthermore, Larson et al. [33] demonstrated in their CT-based study that the presence of a crossover sign (53 %; 95 % CI, 46–60 %) and a positive posterior wall sign (20 %; 95 % CI, 15–26 %) were frequent findings in a young asymptomatic cohort and may very well be a normal variant rather than pathologic.

#### 4.2.5 Femoral Head Morphology

On AP and different lateral views, the femoral head sphericity and offset should be assessed. A Mose template [34] is a template, where concentric circles are used as reference for measuring head sphericity. As a rudimentary guideline, if the femoral epiphysis extends beyond the reference circle margin by >2 mm, the head is considered aspherical. If the femoral epiphysis does not extend beyond 2 mm, then the femoral head is considered spherical [34, 35]. Deviations in head sphericity may be observed not only in FAI but also in avascular necrosis (secondary to segmental collapse) and as sequelae of residual childhood hip conditions such as Legg-Calve-Perthes disease and slipped capital femoral epiphysis (SCFE).

#### 4.2.6 Head-Neck Junction and Offset

On all the views, one can appreciate the femoral head-neck junction and analyze the relationship of the radius of curvature anteriorly versus posteriorly. Clohisy et al. [8] described that a head-neck junction is said to have symmetric concavity, when both the anterior and posterior concavities are symmetric. Otherwise, if the concavity at the anterior aspect of the head-neck junction has a radius of curvature that is greater than that at the posterior aspect of the head-neck junction, the hip is considered to have a moderate decrease in terms of head-neck offset. Finally, if the anterior aspect of the head-neck junction has a convexity, as opposed to a concavity, the head-neck junction is considered to have a prominence (i.e., a “CAM” lesion). Peelle et al. [36] calculated the head-neck offset ratio, which can be measured on lateral radiographs. It is the ratio of three lines: the first is through the center of the long axis of the femoral neck; the second is parallel to the first line, through the most anterior aspect of the femoral neck; the third line is parallel to the second line, through the most anterior aspect of the femoral head. The distance between the second and third line is then divided by the diameter of the femoral head, the normal being an absolute value of  $\geq 9$  mm or a

ratio of the head diameter of  $\geq 0.17$  [37]. A ratio of  $< 0.17$  indicates that a CAM deformity is likely present [36] (ICC=0.86; range=0.76–0.92) [17].

Nötzli et al. [38] described the alpha angle, which is a measurement of femoral head-neck dysplasia, in other words, CAM-type impingement. Originally it was measured on magnetic resonance imaging (MRI) axial views, but can also be calculated on a lateral-type radiograph. It is calculated by measuring the angle between a line drawn from the center of the femoral head to the point of the anterolateral aspect of the head-neck junction where the contour of the femoral head loses its sphericity and the prominence starts (i.e., where the radius of the femoral head begins to increase beyond the radius found more centrally in the acetabulum where the head is more spherical). Originally, the reported average value was  $42^\circ$  (range= $33\text{--}48^\circ$ ) in normal controls (ICC=0.84; range=0.72–.091) [17], compared with  $74^\circ$  (range= $55\text{--}95^\circ$ ) in patients with symptomatic FAI [38–40]. Several threshold values have been suggested to describe when the alpha angle indicates a pathologic entity that may benefit from surgery [8, 41–43]. The most widely accepted threshold angle is  $55^\circ$  and is considered to be indicative of CAM impingement [25] (ICC=0.19; range= $-0.43\text{--}0.54$ ) [17]. Inter- and intra-rater reliability with FAI parameters measured on conventional radiographs is reportedly poor in several studies [8, 29, 44]. Lohan et al. [45] found in their retrospective analysis of MR arthrographic studies that the alpha angle measurement was statistically of no value in suggesting the presence or absence of CAM-type FAI with an up to 30% of the mean value intra-observer variability between the first and second alpha angle measurements for each of their 78 subjects (mean sensitivity=39.3%; mean specificity=70.1%).

#### 4.2.7 Degree of Osteoarthritis (OA)

The Tönnis OA grade can be used to quantify the degree of OA in the impinging hip and can be seen on all views. The scale ranges from 0, which is normal (no signs of OA), to 1, which is mild (increased sclerosis, slight joint space narrowing, no or slight loss of head sphericity), to 2, which is

**Table 4.1** Tönnis osteoarthritis grading scale

Grade	Characteristics
0 – Normal	Absence of signs of OA
1 – Mild	Increased sclerosis Slight joint space narrowing No or slight loss of head sphericity
2 – Moderate	Small cysts Moderate joint space narrowing Loss of head sphericity
3 – Severe	Large cysts Severe joint space narrowing Loss of head sphericity

moderate (small cysts, moderate joint space narrowing, and loss of head sphericity), to 3, which is severe (large cysts, severe joint space narrowing, and loss of head sphericity) [19] (Table 4.1).

## 4.3 Additional Imaging

### 4.3.1 Fluoroscopy

Intraoperative fluoroscopy has been advocated by many and proven to be extremely valuable. It is an essential tool to direct osteochondroplasty intraoperatively. It aids in quantifying the location, configuration, and extent of the CAM lesion prior to the resection and in judging the adequacy of the resection thereafter. Unfortunately, it is the senior author's experience that the same concept does not often apply for pincer lesions, as a true AP radiograph can be difficult to replicate fluoroscopically on the operating table.

Larson and Wulf [46] described a reproducible and systematic intraoperative fluoroscopic evaluation of the hip for the management of CAM and pincer deformities during arthroscopic treatment of FAI. Ross et al. [47] found that their six (6) intraoperative fluoroscopic views allowed further confirmation of bony resection and helped avoid inadequate resections with resultant impingement. They stated that their intraoperative fluoroscopic views are reproducible and could prove to be critical in the absence of a preoperative 3D CT scan.

Although recent studies have demonstrated that fluoroscopy-assisted hip arthroscopy entails safe levels of radiation [48, 49], some may argue that our fluoroscopic views – in addition to

preoperative radiographs and CT – may generate summative doses of radiation that could be avoided. Budd et al. [48] determined on 50 consecutive hip arthroscopies that the mean total fluoroscopy time was 1.10 min and the mean dose area product value was 297.2 cGycm<sup>2</sup> and concluded that a low maximum dose of radiation was achieved and supports its safe use. Gaymer et al. [49] calculated the maximal theoretical risk to a fetus on 166 hip arthroscopies in women of childbearing age. They found that the maximal theoretical dose was 2.99 mGy to the fetus, which places the procedure as low-risk category.

### 4.3.2 Computed Tomography (CT)

The diagnosis and treatment of CAM-type FAI rely on the radiographic identification of deformity and correction of the 3-dimensional (3D) asphericity and loss of offset at the femoral head-neck junction, respectively. Advanced imaging allows for a 3D understanding of the correction needed, but does not necessarily facilitate the intraoperative localization in the absence of navigated instrumentation [38]. Although a considerable ionizing radiation exposure risk is to be taken into account, high-resolution computed tomography (CT) has allowed for increased precision and better definition of osseous morphology of the hip.

### 4.3.3 Magnetic Resonance Imaging (MRI)

Magnetic resonance imaging (MRI) is the preferred modality for the investigation of intra-articular hip pathology [50]. Several studies have demonstrated evidence of MR findings in acetabular labra in asymptomatic volunteers. In 200 asymptomatic hips, Lecouvert et al. [51] found a homogenous low-intensity signal in 44 % of labra, which seemed to decrease significantly with age. Conversely, they also found that the frequency of heterogeneous signal intensities increased with age in 42 % of cases. Cotten et al. [52] later showed in 52 asymptomatic hips that intralabral regions of intermediate or high

signal intensity were found in 57 % of hips. Abe et al. [53] detected similar findings, where in 56 % of their labral segments of 71 asymptomatic hips, homogenous low signal intensity was detected.

Although the demonstration of labral abnormality on an MRI is not essential to the diagnosis of FAI, it does likely indicate the sequelae of the condition in those who have intra-articular hip pain and findings on other imaging modalities consistent with impingement.

Mintz et al. [54] found a sensitivity of 96 %, a specificity of 33 %, and an overall accuracy of 94 % for the detection of labral tears at 1.5 T. Sundberg et al. [55] found comparable results for the detection of labral tears comparing 3-T non-arthrographic with 1.5-T arthrographic techniques. Nowadays, non-contrast MRI is suboptimal for evaluating cartilage and labrum; however, with the development of stronger magnet MRs, this evaluation is improving. It still remains that an MR of the hip, which is a small field of view focus, is more sensitive than an MR of the pelvis, which has a larger field of view.

Magnetic resonance arthrography (MRA) has emerged as the optimal modality for evaluating labrum and cartilage. Compared with hip arthroscopy as gold standard, direct MRA is reported to have sensitivity of 63–100 %, specificity of 44–100 %, and accuracy values of 65–96 % [56–59]. For the detection of labral tears, the interobserver reliability has been reported to be moderate [55–59]. Byrd et al. [5] found in a comparative study between MRI and direct MRA that the clinical assessment can accurately determine the existence of intra-articular hip pathology but is often poor at defining its etiology. An MRI variably shows intra-articular damage with a 42 % false-negative rate. An MRA is found to be more sensitive, but with doubling false-positive interpretation rates. Both studies demonstrated poor reliability in assessing articular damage, but when identified, these studies were 100 % specific. Toomayan et al. [57] found in their sensitivity evaluation of acetabular labral tears in 51 hips that conventional MRI with large field of view was only 8 % sensitive, while conventional MRI

with small field of view was only 25% sensitive in detecting labral tears. In contrast, MRA with small field of view was 92% sensitive in detecting acetabular labral tears. This study highlighted the importance of both small field of view and intra-articular contrast material in the accurate diagnosis of labral abnormalities.

#### 4.4 The Interobserver and Intra-observer Reliability

The interobserver and intra-observer reliabilities of radiographic hip measurements are quite variable in the literature. Clohisy et al. [60] reported poor agreement among 6 hip surgeons. More recent studies have shown more promising results [9, 61]. Mast et al. [61] found an interobserver reliability varying between 0.45 and 0.97 and an intra-observer reliability ranging from 0.55 to 1.0 for common hip measurements. Ayeni et al. [17] recently showed a low reliability between radiologists and orthopedic surgeons in diagnosing FAI pathology on radiographs using standard hip measurements. There was however, a higher interobserver reliability within each specialty ranging from fair to good (ICC=0.59–0.74 and ICC=0.70–0.72, respectively). Orthopedic surgeons had the highest interobserver reliability when identifying pistol grip deformities (ICC=0.81) or abnormal alpha angles (ICC=0.81). These large ranges of interobserver results have pushed for an increased use in advanced imaging with computed tomography (CT) scans and added 3-dimensional (3D) reconstructive views, as well as magnetic resonance imaging (MRI).

#### 4.5 Cost-Utility of Imaging for FAI

The use of imaging is essential in the operative treatment of FAI; however, time and cost of all the diagnostic testing have not been extensively investigated. Kahlenberg et al. [62] studied the average number of health-care providers seen, as well as the average number of diagnostic imaging tests ordered on 78 patients, and then calculated

the average total amount spent per patient prior to diagnosis of FAI. They calculated the minimum cost of diagnosis (AP pelvic and lateral hip radiographs and an MRI, including a visit to an orthopedic surgeon) to be US\$ 690.62 and the average total amount spent per patient in their cohort US\$ 2,456.97, which amounts to US\$ 1,766.35 higher than the calculated minimum cost. They also found that the average duration between onset of symptoms and diagnosis of a labral tear was 32.0 months. It is important for all health-care professionals to recognize and appropriately manage or refer these patients, not only to lower cost but more so to avoid the loss of economic productivity on a societal level.

#### Conclusion

The association between the radiographic findings of femoroacetabular impingement, the correction thereof, and the impact of diagnosis and treatment of the condition on long-term function and prognosis still remain uncertain. Further investigations are required to better define and quantify the diagnostic criteria and thresholds for intervention.

#### Take-Home Points

1. FAI remains predominantly a radiographic diagnosis in symptomatic patients, which justifies the need for imaging in order to appropriately assess the severity and location of lesions associated with FAI.
2. The essential radiograph for the diagnosis of pincer-type FAI is the AP pelvis on which the center-edge angle and crossover sign can be assessed. Both these parameters have exhibited moderate intra- and interobserver reliability, as well as acceptable sensitivity and specificity.
3. A radiograph for the diagnosis of CAM-type FAI is the Dunn lateral view, on which the alpha angle can be assessed. This parameter has demonstrated good intra- and interobserver



reliability, as well as good sensitivity and specificity.

4. Computed tomography (CT) (especially 3D reconstructions) can help further define bony morphology around the hip and better characterize and confirm FAI subtypes and surgical indications. Concerns regarding increased radiation exposure with CT have led to improvements in the technique.
5. Magnetic resonance imaging (MRI) (with or without arthrography, MRA) is a useful adjunct to plain radiographs and CT in assessing the sequelae of FAI, specifically edema patterns, cartilage, and labral lesions.

#### Key Evidence Related Sources

1. Byrd JW, Jones KS. Diagnostic accuracy of clinical assessment, magnetic resonance imaging, magnetic resonance arthrography, and intra-articular injection in hip arthroscopy patients. *Am J Sports Med.* 2004;32(7):1668–74.
2. Clohisy JC, Carlisle JC, Beaulé PE, et al. A systematic approach to the plain radiographic evaluation of the young adult hip. *J Bone Joint Surg Am.* 2008;90 Suppl 4:47–66.
3. Ayeni RO, Chan K, Whelan DB, Gandhi R, Williams D, Harish S, Choudur H, Chiavaras MM, Karlsson J, Bhandari M. Diagnosing femoroacetabular impingement from plain radiographs: do radiologists and orthopaedic surgeons differ? *Orthop J Sports Med.* 2014;2:7.
4. Tannast M, Siebenrock KA, Anderson SE. Femoroacetabular impingement: radiographic diagnosis – what the radiologist should know. *AJR Am J Roentgenol.* 2007;188(6):1540–52.
5. Zaltz I, Kelly BT, Hetsroni I, Bedi A. The crossover sign overestimates acetabular retroversion. *Clin Orthop Relat Res.* 2013;471(8):2463–70.

## References

1. Ganz R, Parvizi J, Beck M, Leunig M, Notzli H, Siebenrock KA. Femoroacetabular impingement: a cause for osteoarthritis of the hip. *Clin Orthop Relat Res.* 2003;417:112–20.
2. McCarthy JC, Noble PC, Schuck MR, Wright J, Lee J, The Otto E. Aufranc Award: the role of labral lesions to development of early degenerative hip disease. *Clin Orthop Relat Res.* 2001;393:25–37.
3. Philippon MJ, Briggs KK, Yen YM, Kuppersmith DA. Outcomes following hip arthroscopy for femoroacetabular impingement with associated chondrolabral dysfunction: minimum two-year follow-up. *J Bone Joint Surg Br.* 2009;91(1):16–23.
4. Beck M, Kalhor M, Leunig M, Ganz R. Hip morphology influences the pattern of damage to the acetabular cartilage: femoroacetabular impingement as a cause of early osteoarthritis of the hip. *J Bone Joint Surg Br.* 2005;87(7):1012–8.
5. Byrd JW. Physical examination. In: *Operative hip arthroscopy.* New York: Springer; 2005. p. 36–50.
6. Parvizi J, Leunig M, Ganz R. Femoroacetabular impingement. *J Am Acad Orthop Surg.* 2007;15(9):561–70.
7. Byrd JW, Jones KS. Diagnostic accuracy of clinical assessment, magnetic resonance imaging, magnetic resonance arthrography, and intra-articular injection in hip arthroscopy patients. *Am J Sports Med.* 2004;32(7):1668–74.
8. Clohisy JC, Carlisle JC, Beaulé PE, et al. A systematic approach to the plain radiographic evaluation of the young adult hip. *J Bone Joint Surg Am.* 2008;90 Suppl 4:47–66.
9. Jamali AA, Mladenov K, Meyer DC, et al. Anteroposterior pelvic radiographs to assess acetabular retroversion: high validity of the “cross-over-sign.” *J Orthop Res.* 2007;25:758–65.
10. Reynolds D, Lucas J, Klaue K. Retroversion of the acetabulum: a cause of hip pain. *J Bone Joint Surg Br.* 1999;81(2):281–8.
11. Dunn DM. Anteversion of the neck of the femur; a method of measurement. *J Bone Joint Surg Br.* 1952;34:181–6.
12. Meyer DC, Beck M, Ellis T, Ganz R, Leunig M. Comparison of six radiographic projections to assess femoral head/neck asphericity. *Clin Orthop Relat Res.* 2006;445:181–5.
13. Clohisy JC, Nunley RM, Otto RJ, Schoenecker PL. The frog-leg lateral radiograph accurately visualized hip cam impingement abnormalities. *Clin Orthop Relat Res.* 2007;462:115–21.
14. Lequesne M, de Seze. False profile of the pelvis. A new radiographic incidence for the study of the hip. Its use in dysplasias and different coxopathies. *Rev Rhum Mal Osteoartic.* 1961;28:643–52. French.
15. Siebenrock KA, Kalbermatten DF, Ganz R. Effect of pelvic tilt on acetabular retroversion: a study of pelvis from cadavers. *Clin Orthop Relat Res.* 2003;407:241–8.

16. Pullen W, Henebry A, Gaskill T. Variability of acetabular coverage between supine and weight-bearing pelvic radiographs. *Am J Sports Med.* 2014;42(11):2643.
17. Ayeni RO, Chan K, Whelan DB, Gandhi R, Williams D, Harish S, Choudur H, Chiavaras MM, Karlsson J, Bhandari M. Diagnosing femoroacetabular impingement from plain radiographs: do radiologists and orthopaedic surgeons differ? *Orthop J Sports Med.* 2014;2:7.
18. Nepple JJ, Lehmann CL, Ross JR, Schoenecker PL, Clohisy JC. Coxa profunda is not a radiographic parameter for diagnosing pincer-type femoroacetabular impingement. *J Bone Joint Surg Am.* 2013;95(5):417–23.
19. Tönnis D. Congenital dysplasia and dislocation of the Hip in children and adults. Heidelberg/Germany: Springer; 1987.
20. Wiberg G. Studies on dysplastic acetabula and congenital subluxation of the hip: with special reference to the complication of osteoarthritis. *Acta Chir Scand Suppl.* 1939;58:7–38.
21. Monazzam S, Bomar JD, Cidambi K, Kruk P, Hosalkar H. Lateral center-edge angle on conventional radiography and computed tomography. *Clin Orthop Relat Res.* 2013;471(7):2233–7.
22. Murphy SB, Ganz R, Muller ME. The prognosis in untreated dysplasia of the hip: a study of radiographic factors that predict the outcome. *J Bone Joint Surg Am.* 1995;77:985–9.
23. Murphy SB, Kijewski PK, Millis MB, Harless A. Acetabular dysplasia in the adolescent and young adult. *Clin Orthop Relat Res.* 1990;261:214–23.
24. Werner CM, Ramseier LE, Ruckstuhl T, Stromberg J, Copeland CE, Turen CH, Rufibach K, Bouaicha S. Normal values of Wiberg's lateral center-edge angle and Lequesne's acetabular index: a coxometric update. *Skeletal Radiol.* 2012;41:1273–8.
25. Tannast M, Siebenrock KA, Anderson SE. Femoroacetabular impingement: radiographic diagnosis – what the radiologist should know. *AJR Am J Roentgenol.* 2007;188(6):1540–52.
26. Colvin AC, Koehler SM, Bird J. Can the change in center-edge angle during pincer trimming be reliably predicted? *Clin Orthop Relat Res.* 2011;469:1071–4.
27. Kutty S, Schneider P, Faris P, Kiefer G, Frizzell B, Park R, Powell JN. Reliability and predictability of the centre-edge angle in the assessment of pincer femoroacetabular impingement. *Int Orthop.* 2012;36:505–10.
28. Philippon MJ, Wolff AB, Briggs KK, Zehms CT, Kuppersmith DA. Acetabular rim reduction for the treatment of Femoroacetabular impingement correlates with preoperative and postoperative center-edge angle. *Arthroscopy.* 2010;26:757–61.
29. Carlisle JC, Zebala LP, Shia DS, et al. Reliability of various observers in determining common radiographic parameters of adult hip structural anatomy. *Iowa Orthop J.* 2011;31:52–8.
30. Anderson LA, Peters CL, Park BB, Stoddard GJ, Erickson JA, Crim JR. Acetabular cartilage delamination in femoroacetabular impingement: risk factors and magnetic resonance imaging diagnosis. *J Bone Joint Surg Am.* 2009;91(2):305–13.
31. Kalberer F, Sierra RJ, Madan SS, Ganz R, Leunig M. Ischial spine projection into the pelvis: a new sign for acetabular retroversion. *Clin Orthop Relat Res.* 2008;466(3):677–83.
32. Zaltz I, Kelly BT, Hetsroni I, Bedi A. The crossover sign overestimates acetabular retroversion. *Clin Orthop Relat Res.* 2013;471(8):2463–70.
33. Larson CM, Moreau-Gaudry A, Kelly BT, Byrd JW, Tonetti J, Lavallee S, Chabanas L, Barrier G, Bedi A. Are normal hips being labeled as pathologic? A CT-based method for defining normal acetabular coverage. *Clin Orthop Relat Res.* 2015;473(4):1247–54.
34. Mose K. Methods of measuring in Legg-Calvé-Perthes disease with special regard to the prognosis. *Clin Orthop Relat Res.* 1980;150:103–9.
35. Weinstein SL. Legg-Calvé-Perthes disease. In: Morrissy RT, editor. Lovell and Winter's pediatric orthopaedics. 3rd ed. Philadelphia: Lippincott; 1990. p. 867–8.
36. Peelle MW, Della Rocca GJ, Maloney WJ, Curry MC, Clohisy JC. Acetabular and femoral radiographic abnormalities associated with labral tears. *Clin Orthop Relat Res.* 2005;441:327–33.
37. Maheshwari AV, Malik A, Dorr LD. Impingement of the native hip joint. *J Bone Joint Surg Am.* 2007;89:2508–18.
38. Notzli HP, Wyss TF, Stoecklin CH, Schmid MR, Treiber K, Hodler J. The contour of the femoral head-neck junction as a predictor for the risk of anterior impingement. *J Bone Joint Surg Br.* 2002;84(4):556–60.
39. Beaulé PE, Zaragoza E, Motamedi K, Copelan N, Dorey FJ. Three-dimensional computed tomography of the hip in the assessment of femoroacetabular impingement. *J Orthop Res.* 2005;23(6):1286–92.
40. Johnston TL, Schenker ML, Briggs KK, Philippon MJ. Relationship between offset angle alpha and hip chondral injury in femoroacetabular impingement. *Arthroscopy.* 2008;24(6):669–75.
41. Allen D, Beaulé PE, Ramadan O, Doucette S. Prevalence of associated deformities and hip pain in patients with cam-type femoroacetabular impingement. *J Bone Joint Surg Br.* 2009;91(5):589–94.
42. Gosvig KK, Jacobsen S, Palm H, Sonne-Holm S, Magnusson E. A new radiological index for assessing asphericity of the femoral head in cam impingement. *J Bone Joint Surg Br.* 2007;89(10):1309–16.
43. Tannast M, Siebenrock KA. Conventional radiographs to assess femoroacetabular impingement. *Instr Course Lect.* 2009;58:203–12.
44. Noh MR, Schweitzer ME, Rybak L, Cohen J. Femoroacetabular impingement: can the alpha angle be estimated? *AJR Am J Roentgenol.* 2008;190(5):1260–2.
45. Lohan DG, Seeger LL, Motamedi K, Hame S, Sayre J. Cam-type FAI: is the alpha angle the best

- MR arthrography has to offer? *Skeletal Radiol.* 2010;39(2):203–4.
46. Larson CM, Wulf CA. Intraoperative fluoroscopy for evaluation of bony resection during arthroscopic management of femoroacetabular impingement in the supine position. *Arthroscopy.* 2009;25(10):1183–92.
  47. Ross JR, Bedi A, Stone RM, Sibilsky Enselman E, Leunig M, Kelly BT, Larson CM. Intraoperative fluoroscopic imaging to treat cam deformities: correlation with 3-dimensional computed tomography. *Am J Sports Med.* 2014;42(6):1370–6.
  48. Budd H, Patchava A, Khanduja V. Establishing the radiation risk from fluoroscopic-assisted arthroscopic surgery of the hip. *Int Orthop.* 2012;36(9):1803–6.
  49. Gaymer CE, Achten J, Auckett R, Cooper L, Griffin D. Fluoroscopic radiation exposure during hip arthroscopy. *Arthroscopy.* 2013;29(5):870–3.
  50. Beaulé PE, Zaragoza E, Copelan N. Magnetic resonance imaging with gadolinium arthrography to assess acetabular cartilage delamination: a report of four cases. *J Bone Joint Surg Am.* 2004;86-A:2294–8.
  51. Lecouvet FE, VandeBerg BC, Melghem J, et al. MR imaging of the acetabular labrum: variations in 200 asymptomatic hips. *Am J Roentgenol.* 1996;167:1025–8.
  52. Cotten A, Boutry N, Demondion X, et al. Acetabular labrum: MRI in asymptomatic volunteers. *J Comput Assist Tomogr.* 1998;22:1–7.q.
  53. Abe I, Harada Y, Oinuma K, Kamikawa K, Kitahara H, Morita F, Moriya H. Acetabular labrum: abnormal findings at MR imaging in asymptomatic hips. *Radiology.* 2000;216(2):576–81.
  54. Mintz DN, Hooper T, Connell D, et al. Magnetic resonance imaging of the hip: detection of labral and chondral abnormalities using noncontrast imaging. *Arthroscopy.* 2005;21:385–93.
  55. Sundberg TP, Toomayan GA, Major NM. Evaluation of the acetabular labrum at 3.0-T MR imaging compared with 1.5-T MR arthrography: preliminary experience. *Radiology.* 2006;238:706–11.
  56. Chan YS, Lien LC, Hsu HL, Wan YL, Lee MS, Hsu KY, Shih CH. Evaluating hip labral tears using magnetic resonance arthrography: a prospective study comparing hip arthroscopy and magnetic resonance arthrography diagnosis. *Arthroscopy.* 2005;21:1250.
  57. Toomayan GA, Holman WR, Major NM, Kozlowski SM, Vail TP. Sensitivity of MR arthrography in the evaluation of acetabular labral tears. *AJR Am J Roentgenol.* 2006;186:449–53.
  58. Freedman BA, Potter BK, Dinauer PA, Giuliani JR, Kuklo TR, Murphy KP. Prognostic value of magnetic resonance arthrography for Czerny stage II and III acetabular labral tears. *Arthroscopy.* 2006;22:742–7.
  59. Keeney JA, Peelle MW, Jackson J, et al. Magnetic resonance arthrography versus arthroscopy in the evaluation of articular hip pathology. *Clin Orthop Relat Res.* 2004;(429):163–9.
  60. Clohisy JC, Carlisle JC, Trousdale R, et al. Radiographic evaluation of the hip has limited reliability. *Clin Orthop Relat Res.* 2009;467(3):666–75.
  61. Mast NH, Impellizzeri F, Keller S, Leunig M. Reliability and agreement of measures used in radiographic evaluation of the adult hip. *Clin Orthop Relat Res.* 2011;469:188–99.
  62. Kahlenberg CA, Han B, Patel RM, Deshmans PP, Terry MA. Time and cost of diagnosis for symptomatic femoroacetabular impingement. *Orthop J Sports Med.* 2014;2(3):2325967114523916.